PATTERN FORMATION IN UNCATALYZED BROMATE OSCILLATOR WITH PYROGALLOL

Ľubica ADAMČÍKOVÁ[1,]*, Róbert BIELIK[2] and Peter ŠEVČÍK[3]

Department of Physical and Theoretical Chemistry, Comenius University,
842 15 Bratislava, Slovak Republic; e-mail: [1] adamcikova@fns.uniba.sk, [2] bielik@fns.uniba.sk,
[3] sevcik@fns.uniba.sk

Received March 16, 2004
Accepted April 30, 2004

Stationary mosaic and trigger wave patterns may spontaneously develop in an unstirred thin film of solution containing bromate, pyrogallol and sulfuric acid (uncatalyzed bromate system). The propagation velocity of the waves was found to depend not only on the initial concentrations of H^+ and BrO_3^- ions but also on the initial concentration of pyrogallol. For the explanation of the wave velocity dependence, a reaction scheme of the pyrogallol–BrO_3^- system has been proposed. The scheme is based on the well-known bromate chemistry combined with an organic radical control that takes into account the reactions of pyrogallol with BrO_3^-, $HBrO_2$ and HOBr. Movement of the waves could be recorded also potentiometrically. The kinetics and mechanism of the reaction between pyrogallol and bromate in an H_2SO_4 medium were studied using a conventional polarographic method.

Keywords: Uncatalyzed bromate oscillator; Bromate; Pyrogallol; Pattern formation; Kinetics; Potentiometry; Belousov–Zhabotinsky reaction; Polarography.

Nonlinear chemical dynamics has grown rapidly, perhaps exponentially, during the past three decades. Many of the most exciting recent developments in chemistry involve the phenomenon of self-organization[1,2]. Spatial concentration patterns arise from the coupling of a nonlinear chemical reaction with diffusion and/or flow. In many chemical and biological systems, the underlying nonlinearity is caused by autocatalysis that can spread through an extended system via the diffusion of the corresponding autocatalytic species[3].

The widely studied experimental system is the Belousov–Zhabotinsky (BZ) reaction[4]. This reaction involves oxidation of an organic substrate with bromate in the presence of a catalyst, for example a Fe(II) complex of phenanthroline (ferroin). The intermediate $HBrO_2$ is the autocatalytic species that determines the propagation velocity of the front depending on its rate of production and diffusion constant. Concentric blue rings, known as tar-

doi:10.1135/cccc20041553

get patterns, can develop spontaneously in the initially homogeneous red solution and propagate outwards from their centers. The recovery process in the wake of the front is controlled by a decrease in the bromide concentration due to the reaction, which leads the system back from the oxidized to the reduced state. Electrochemical detection of the pattern formation in the BZ reaction was carried out by Nagy-Ungvarai et al.[5] In the BZ system with pyrogallol as substrate and ferroin as catalyst, a saturation-type relationship in the propagation velocity dependence on electric field intensity has been found, unlike in the classic BZ system[6]. It has been found that the wave velocity in the metal-ion catalyzed BZ reaction–diffusion system is linearly dependent on the square root of the product of proton and bromate ion concentrations and is independent of the concentrations of the catalyst and organic substrate[7,8].

The uncatalyzed class of bromate oscillators (UBO) does not require any metal-ion catalyst and the aromatic organic substrate (mostly phenol or aniline derivatives) performs some of the functions of the metal ion as well[9,10]. A quinone derivative of the original organic reactant is produced in a two-electron oxidation process involving oxygen-bromine species (mainly BrO_3^- and HOBr). The quinone then plays the role of the traditional, one-electron-transfer catalyst. In UBO systems, stationary and moving structures were observed[11–14]. Intensely colored intermediates form periodically during the reaction and allow visual observation of the structure. A major advantage of the UBO systems is the lack of CO_2 production, thereby being convenient for studying pattern formation. In UBO systems, formation of $HBrO_2$ cannot be accompanied by oxidation of the metal-ion catalyst.

In the present paper, we report on an uncatalyzed BZ system with a reductant pyrogallol (1,2,3-trihydroxybenzene). The same system was studied by Sridevi and Ramaswamy[13], but in the presence of ferroin as a catalyst. When a catalyst is added, UBO systems become internally coupled (via oxygen-bromine intermediates) with the classic BZ system, which leads to significant changes in the behavior of the system.

EXPERIMENTAL

All chemicals were of commercial analytical quality and were used without further purification. Doubly ion-exchanged water was used throughout.

The patterns were studied in a Petri dish with the inner diameter 8.9 cm, height 1.9 cm and with the depth of the liquid layer 1.6 mm, unless indicated otherwise. The solution depth was calculated from the reaction mixture volume (10 cm^3) and the area of the Petri dish (62.6 cm^2). The calculated depths are only approximate, as no attempt was made to correct for the solution adhered to the Petri dish sides by capillary action. The solution was photographed at known times by an Olympus Camedia C-3000 Zoom camera.

The kinetics of oxidation of pyrogallol (PG) with bromate ions was studied polarographically by recording the time dependence of the limiting diffusion current of BrO_3^- ions at –1.0 V against a reference mercury(I) sulfate electrode (MSE). Measurements were made in a Kalousek cell with a thermostated mantle, using a mercury dropping electrode. The temperature was kept constant within ±0.1 °C.

The potential signal was measured between a Pt point electrode and the MSE or with a pair of Pt point electrodes in a thin layer of unstirred solution, using a Radelkis OH-105 polarograph.

^{1}H NMR spectra were recorded on a Varian GEMINY 2000 spectrometer operating at a resonance frequency of 300 MHz, with TMS as internal standard and DMSO as a solvent. The NMR measurements were performed at laboratory temperature.

RESULTS AND DISCUSSION

The spatial behavior was studied with the solution spread over a Petri dish in a thin layer. Two types of pattern formation could be observed in our system.

System A

A thoroughly mixed solution of 2 M H_2SO_4, 0.026 M PG and 0.05 M $NaBrO_3$ was poured into a Petri dish to make a layer of 1.6 mm. The following series of photographs (Figs 1a–1e) show the typical pattern development. First, the transient mosaic pattern was generated (Fig. 1b); later, a pattern of chemical waves – trigger waves appeared (Figs 1d, 1e). At a certain phase of the pattern development, pacemaker centers appeared in the mosaic part of the pattern, from which chemical waves started to propagate (Figs 1b, 1c). The average propagation velocity of the waves was 9.2 ± 0.4 mm/min. The first ring may be initiated by a microscopic concentration or phase fluctuation or by a macroscopic catalytic, nucleating heterogeneous center.

The movement of the waves could also be recorded potentiometrically. The oscillations of the Pt point electrode potential versus the reference MSE or versus the second Pt point electrode were observed in unstirred solutions in the Petri dish (Fig. 2, curves *1*, *2*). The oscillating course was independent of the distance of the electrodes inserted into the solution.

Influence of Control Parameters

Bromate variation. Pattern formation was formed in the concentration range $0.04 < [BrO_3^-]_o < 0.1$ mol/dm^3. Well measurable trigger waves could be observed only in a certain narrow concentration range (0.04–0.06 mol/dm^3), with the wave velocity increased when the bromate concentration increased (Fig. 3). The same trend had the dependence of the frequency of oscillation, measured potentiometrically with increasing concentration of bromate (Fig. 4, curves *1*–*3*). The colored contrast and the symmetry of the transient structure increased with decreasing concentration of bromate.

Sulfuric acid variation. The pattern formation was observed in the concentration range 1.2–3 mol/dm^3. The number of chemical waves and their symmetry increased with increasing concentration of H_2SO_4. When $[H_2SO_4]_o > 2.6$ mol/dm^3, the transient mosaic pattern was suppressed. Color contrast increased with decreasing concentration of H_2SO_4. The wave velocity (Fig. 5) and the frequency of oscillations, measured potentiometrically (Fig. 4, curves *1*–*3*), increased with increasing concentration of H_2SO_4.

Pyrogallol variation. In the classic catalyzed BZ reaction, the wave velocity is almost independent of the substrate concentration. In our UBO system, a

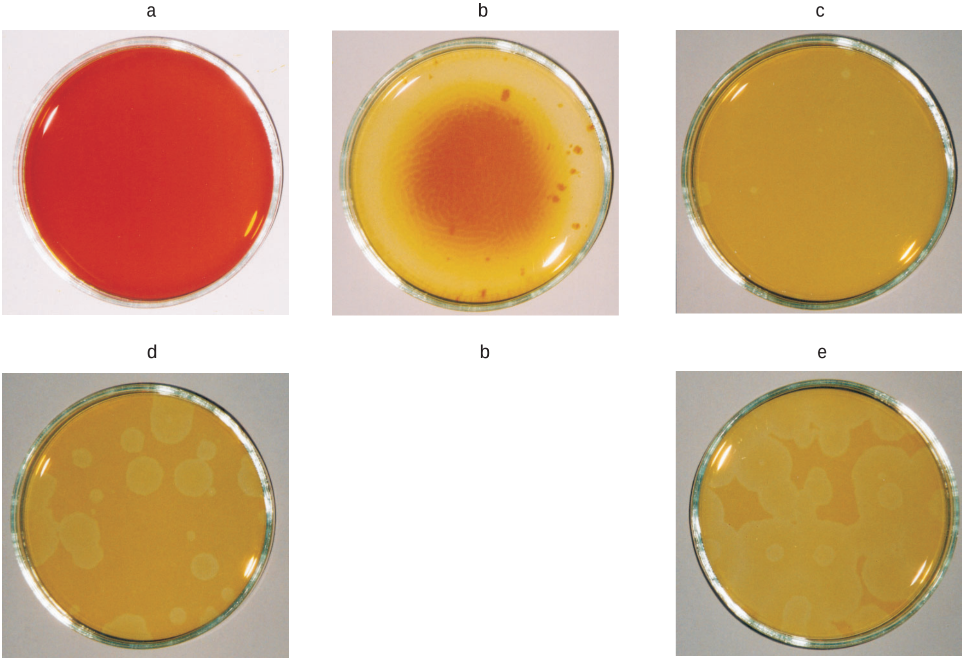

FIG. 1
Photographs demonstrating the generation and propagation of chemical waves. Initial concentrations (in mol/dm^3): $[PG]_o = 0.026$, $[BrO_3^-]_o = 0.05$ and $[H_2SO_4] = 2$. Thickness of the layer, $l = 1.6$ mm. The pictures were taken at 10 (a), 194 (b), 300 (c), 410 (d) and 490 (e) s after starting the experiment

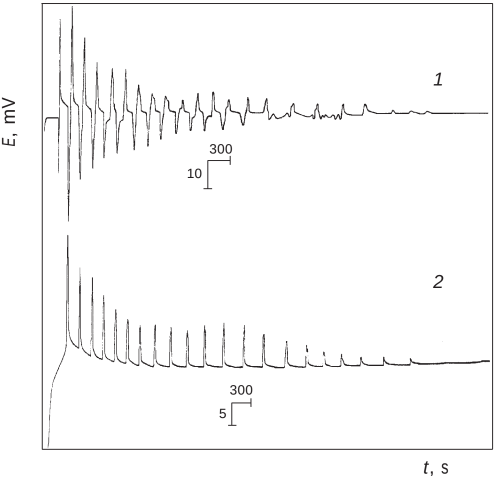

FIG. 2
Potentiometric traces in the thin layers of uncatalyzed PG–bromate solution. The oscillations of the Pt point electrode potential vs the second Pt point electrode (*1*); the oscillations of the Pt point electrode potential vs a reference MSE (*2*). Initial concentrations as in Fig. 1

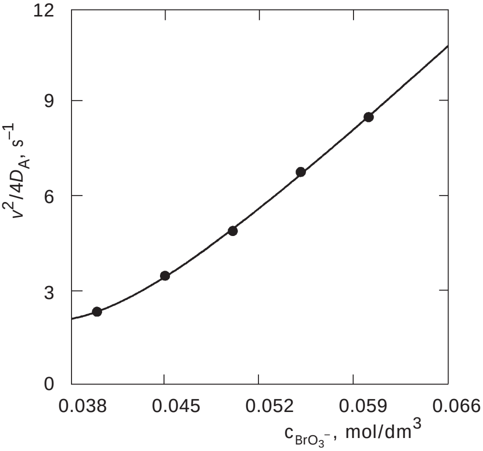

FIG. 3
Dependence of the wave velocity on $[BrO_3^-]_o$. The circles represent the experimental values. The solid line curve is calculated on the basis of Eq. (*15*). Initial concentrations (in mol/dm^3): $[H_2SO_4]_o = 2$ and $[PG]_o = 0.026$. Thickness of the layer, $l = 1.6$ mm

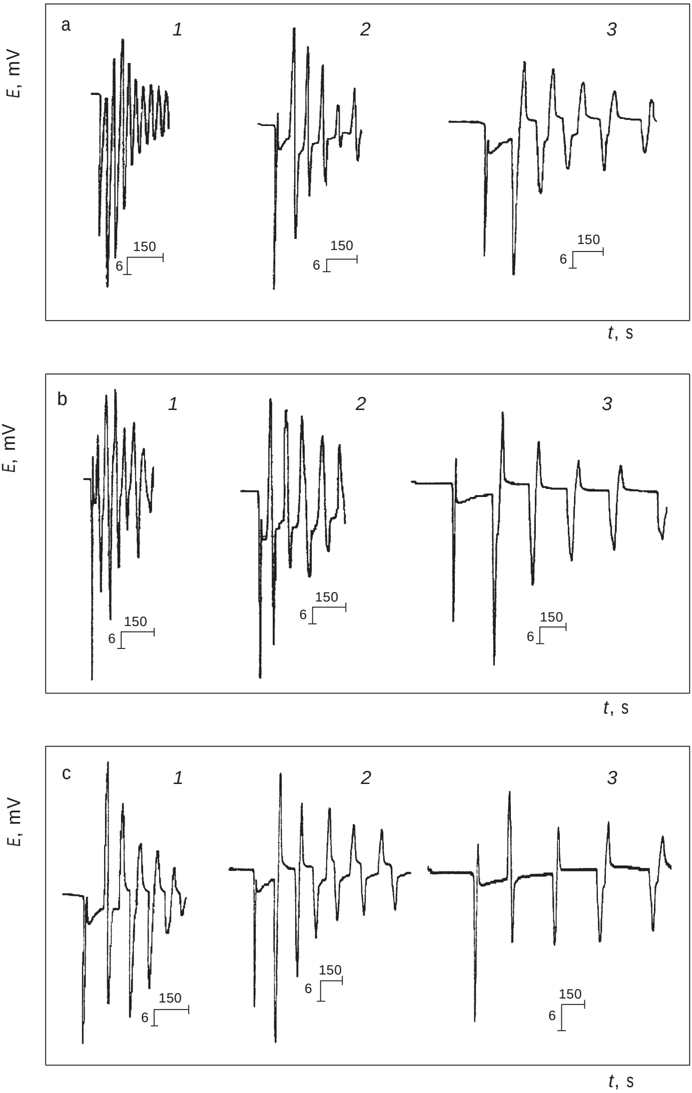

FIG. 4

Potential traces in solution thin layers, l = 1.6 mm, for different PG, H_2SO_4 and bromate concentrations. Initial concentrations (in mol/dm^3): a $[PG]_o$ = 0.026, $[H_2SO_4]_o$ = 2 and $[BrO_3^-]_o$ = 0.09 (*1*), 0.06 (*2*), 0.05 (*3*); b $[PG]_o$ = 0.026, $[BrO_3^-]_o$ = 0.05 and $[H_2SO_4]_o$ = 2.8 (*1*), 2.4 (*2*), 1.8 (*3*); c $[H_2SO_4]_o$ = 2, $[BrO_3^-]_o$ = 0.05 and $[PG]_o$ = 0.02 (*1*), 0.026 (*2*), 0.03 (*3*) rather unexpected observation was made that the propagation velocity of chemical waves strongly depends on the PG concentration. The velocity of wave propagation and the frequency of oscillations in the BrO_3^-–PG–acid system decreased with increasing concentration of PG (Fig. 6 and Fig. 4,

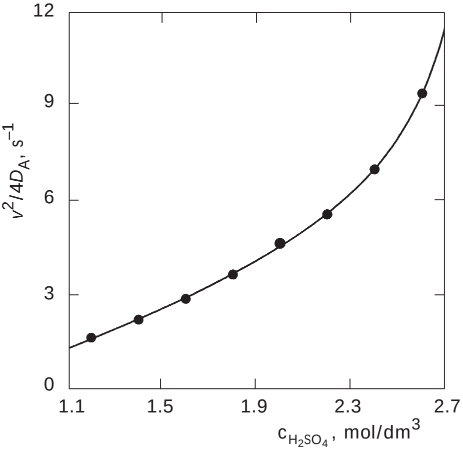

FIG. 5

Dependence of the wave velocity on $[H_2SO_4]_o$. The circles represent the experimental values. The solid line curve is calculated on the basis of Eq. (*15*). Initial concentrations (in mol/dm^3): $[PG]_o = 0.026$ and $[BrO_3^-]_o = 0.05$. Thickness of the layer, $l = 1.6$ mm

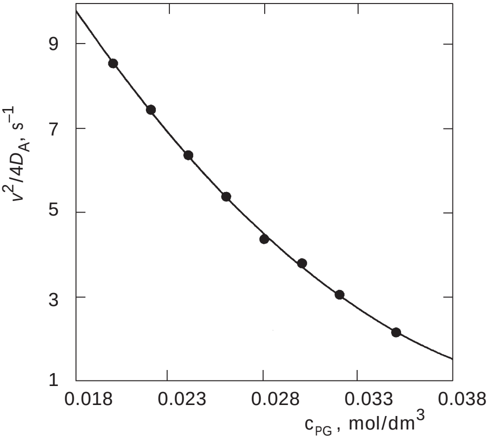

FIG. 6

Dependence of the wave velocity on $[PG]_o$. The circles represent the experimental values. The solid line curve is calculated on the basis of Eq. (*15*). Initial concentrations (in mol/dm^3): $[H_2SO_4]_o = 2$ and $[BrO_3^-]_o = 0.05$. Thickness of the layer, $l = 1.6$ mm curves *1*–*3*). It was found that for $[PG]_o < 0.035$ mol/dm^3, the transient mosaic pattern and trigger waves were observed; the pattern development was that as in Fig. 1. However, when $[PG]_o > 0.04$ mol/dm^3, only a stationary mosaic structure appeared.

The velocity v ($[v]$ = mm/min) of a reaction–diffusion wave in the BZ reaction is primarily determined by the diffusion coefficient D of the autocatalytic species $HBrO_2$ ($D = 1.5 \times 10^{-5}$ cm^2/s) and by the rate constant k_5 of the rate-determining step of the autocatalytic reaction (Eqs (*1*), (*2*)).

$$v = 2(Dk_5[BrO_3^-][H^+])^{1/2} \qquad (1)$$

$$v = 28.8\ ([BrO_3^-][H^+])^{1/2} \qquad (2)$$

This relationship, predicted by Luther, can be derived analytically from a simple model of autocatalysis combined with difussion[15]. Field and Noyes[7] found that the wave velocity in the ferroin-catalyzed BZ reaction was indeed proportional to the product $([BrO_3^-][H^+])^{1/2}$; however, the following relationship gave a better fit with the results (Eq. (*3*)).

$$v = -0.832 + 27.8\ ([BrO_3^-][H^+])^{1/2} \qquad (3)$$

The negative intercept is attributed to the effect of bromide ions in the solution ahead of the wave[8]. More accurate expressions for the velocity dependence of the wave can be obtained by considering the full mechanism instead of the single rate-determining step[16].

Orbán, Körös and Noyes[18] suggested a mechanism to explain the uncatalyzed BZ reaction. Additional modeling studies have been made by Liu and Scott[19].

The organic species are easily oxidized, playing the role of the metal catalyst[17,18]. For example, pyrogallol can replace the metal catalyst in the reaction with $BrO_2^\bullet$:

$$BrO_2^\bullet + C_6H_3(OH)_3 \longrightarrow HBrO_2 + C_6H_3(OH)_2O^\bullet\ . \qquad (4)$$

In our uncatalyzed PG–BrO_3^- system, we found deviations from a linear dependence of the wave velocity on $([BrO_3^-][H^+])^{1/2}$. A very significant part of our experiment is the dependence of the wave velocity on the concentration of pyrogallol. Pyrogallol is easily oxidized with BrO_3^- in acid media; kinetics and mechanism of this reaction are described later.

The observed experimental features can be reproduced numerically on the basis of a simplified reaction scheme for the PG–BrO_3^- system (Eqs (*5*)–(*14*)):

$$BrO_3^- + Br^- + 2\ H^+ \rightleftharpoons HBrO_2 + HBrO \tag{5}$$

$$HBrO_2 + Br^- + H^+ \longrightarrow 2\ HBrO \tag{6}$$

$$BrO_3^- + HBrO_2 + H^+ \rightleftharpoons 2\ BrO_2^{\bullet} + H_2O \tag{7}$$

$$BrO_2^{\bullet} + R \longrightarrow HBrO_2 + R^{\bullet} \tag{8}$$

$$BrO_2^{\bullet} + R^{\bullet} \longrightarrow HBrO_2 + Q \tag{9}$$

$$2\ HBrO_2 \longrightarrow BrO_3^- + HBrO + H^+ \tag{10}$$

$$HBrO_2 + R \longrightarrow HBrO + Q + H_2O \tag{11}$$

$$HBrO + R \longrightarrow Br^- + H^+ + Q + H_2O \tag{12}$$

$$BrO_3^- + R + 2\ H^+ \longrightarrow HBrO_2 + Q + H^+ + H_2O \tag{13}$$

$$HBrO_2 + R^{\bullet} \longrightarrow HBrO + Q^{\bullet} + H_2O\ , \tag{14}$$

where R is pyrogallol and Q is 3-hydroxy-1,2-benzoquinone.

The mathematical analysis of the model with an additional quasisteady-state approximation for the radical intermediates, with addition of diffusion terms to the differential equations and with $D_{\mathrm{HBrO2}} = 1.5 \times 10^{-5}$ cm^2/s, gives the following equation:

$$\frac{v^2}{4D_A} = k_3[H^+][BrO_3^-] - k_2[H^+][Br^-] - k_7[R] - \frac{2k_3k_4k_{10}[H^+][BrO_3^-][R]}{2k_3k_5[H^+][BrO_3^-] + k_4k_{10}[R]}, \tag{15}$$

where D_A is the diffusion coefficient of the autocatalytic species $HBrO_2$.

This equation describes the wave velocity as a function of reactant concentrations and relatively good agreement with experiment was obtained (Figs 3, 5 and 6).

Dependence on Fluid Layer Depth

Both transient mosaic pattern and trigger waves are dependent on the depth of fluid layer. Figures 7a–7c indicate the change of the dot size of the mosaic pattern with increasing depth of the fluid. The dependence wave propagation velocity on the layer thickness has a sigmoidal shape.

Wave Velocity as a Function of Temperature

The velocity of trigger waves was measured in the temperature range 9–31.5 °C, with the following system composition: $[BrO_3^-]_o = 0.05$ mol/dm^3, $[PG]_o = 0.026$ mol/dm^3, $[H_2SO_4]_o = 2$ mol/dm^3. The temperature dependence of the velocity v can be described by the Arrhenius relationship $\ln v \approx -E_a/RT$, where E_a is an apparent activation energy, R is the gas constant ant T is temperature (K). Linear regression analysis yields $E_a = 33.5$ kJ/mol. This value is very similar to activation energy values for catalyzed BZ waves[20].

System B

A stationary mosaic pattern (without trigger waves) was observed for 0.07 M PG, 0.05 M BrO_3^- and 2 M H_2SO_4 ($c_{PG} > c_{BrO3-}$); the evolution of the pattern was analogous to that in the phenol–bromate or pyrocatechol–bromate sys-

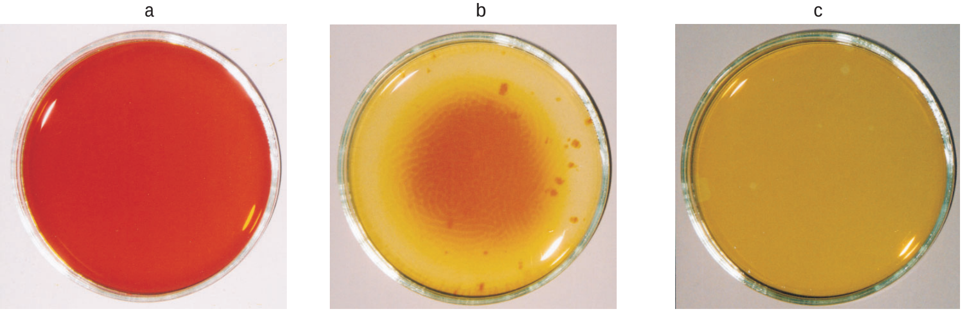

FIG. 7
Typical patterns obtained by increasing the depth of the fluid layer. Initial concentrations as in Fig. 1. Thickness of the layer, l (in mm): 0.8 (a), 3 (b), 10 (c)

tems[12]. In the beginning, the liquid appears as a homogeneous brown-red fluid layer. After 100 s, a mosaic pattern appears in the undisturbed and uncovered solution and fills the whole Petri dish. After a few minutes, the mosaic pattern breaks into other structures. We can observe from the evolution of the pattern that the arising ring, which borders mosaic pattern, decreases with time and the rate of movement of this ring is $v = 0.8$ mm/min. This structure resembled kiwi fruit, cut up across. The development of the pattern was accompanied by formation of a precipitate. Using UV-VIS and ^1H NMR spectroscopies, 1,7-dibromopurpurogallin was identified as a product of the reaction. This pattern is a result of a coupling of a nonlinear chemical reaction and convection.

Kinetics of the Reaction Between Pyrogallol and Bromate Ion in Sulfuric Acid

When the initial concentration of bromate is at least twice that of pyrogallol, $[BrO_3^-]_o > [PG]_o$, the reaction oscillates in a stirred batch system[21]. Both temporal oscillations in stirred solutions and spatial phenomena under unstirred conditions manifest themselves at the same composition of the reaction mixture. When $[BrO_3^-]_o < [PG]_o$, the concentration of bromate ions decreases exponentially in the course of the reaction. First-order kinetics is well obeyed when the initial concentration of BrO_3^- ions is 5×10^{-4}, that of PG varies from 0.01 to 0.12 and that of H_2SO_4 from 0.5 to 1.5 mol/dm^3. The rate constant of bromate reduction in the presence of excess pyrogallol has been determined from the slope of the linear dependence of $\ln (c_o/c)$ on time. The rate constant increases linearly with the concentration of PG. Logarithmic analysis revealed that the reaction is of the second order with respect to hydrogen ions.

According to the above findings, the experimental rate equation has the form

$$-d[BrO_3^-]/dt = k[BrO_3^-][PG][H_3O^+]^2 \ . \qquad (16)$$

The value of k is 2.56×10^{-2} dm^3/mol s in 1 M H_2SO_4 at 20 °C and at I = 1.9 mol/dm^3 (ionic strength maintained by addition of $NaClO_4$).

The pH dependence, indicating the exchange of two protons and the analogy with the oxidation of tertiary alcohols with bromate[22,23], makes it possible to propose the probable mechanism:

$$BrO_3^- + 2\,H^+ \overset{K}{\rightleftharpoons} H_2BrO_3^+$$

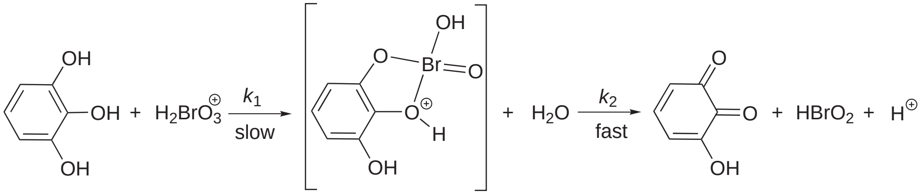

The rate equation derived on this basis is in accord with that found experimentally. The activation parameters of the reaction, determined from the temperature dependence of the rate constant, are $\Delta H^{\ddagger}$ = 64.3 kJ/mol and $\Delta S^{\ddagger}$ = –56 J/K mol. They are comparable with those of the BrO_3^-–gallic acid reaction[22]. The rates of reactions PG + $HBrO_2$ and PG + HOBr are much higher than that of the PG–BrO_3^- reaction.

This work was supported by the Grant Agency of the Ministry of Education of the Slovak Republic (grant No. 1/0050/03).

REFERENCES

1. Kapral R., Showalter K. (Eds): *Chemical Waves and Patterns*. Kluwer, Dordrecht 1995.
2. Epstein I. R., Pojman J. A.: *An Introduction to Nonlinear Chemical Dynamics*. Oxford University Press, New York 1998.
3. Ross J., Müller S. C., Vidal C.: *Science* **1988**, *240*, 460.
4. Field R. J., Burger M.: *Oscillations and Traveling Waves in Chemical Systems*. Wiley-Interscience, New York 1985.
5. Nagy-Ungvarai Zs., Baumgärtl H., Hess B.: *Chem. Phys. Lett.* **1990**, *168*, 539.
6. Pornprompanya M., Müller S. C., Ševčíková H.: *Phys. Chem. Chem. Phys.* **2002**, *4*, 3370.
7. Field R. J., Noyes R. M.: *J. Am. Chem. Soc.* **1974**, *96*, 2001.
8. Kuhnert L., Krug H. J.: *J. Chem. Phys.* **1987**, *91*, 730.
9. Orbán M., Körös E.: *J. Phys. Chem.* **1978**, *82*, 1672.
10. Liu J., Scott S. K.: *J. Phys. Chem.* **1992**, *96*, 9870.
11. Orbán M.: *J. Am. Chem. Soc.* **1980**, *102*, 4311.
12. Adamčíková Ľ., Farbulová Z., Ševčík P.: *React. Kinet. Catal. Lett.* **2002**, *75*, 335.
13. Sridevi V., Ramaswamy R.: *Chem. Lett.* **1998**, *5*, 459.
14. Adamčíková Ľ., Holba V., Parkániová V.: *Collect. Czech. Chem. Commun.* **1995**, *60*, 545.
15. Luther R.: *Elektrochemie* **1906**, *12*, 596.
16. Eager M. D., Santos M., Dolnik M., Zhabotinsky A. M., Kustin K., Epstein I.: *J. Phys. Chem.* **1994**, *98*, 10750.
17. Scott S. K.: *Oscillations, Waves and Chaos in Chemical Kinetics*. Oxford University Press, Oxford 1994.
18. Orbán M., Körös E., Noyes R. M.: *J. Phys. Chem.* **1979**, *83*, 3056.
19. Liu J., Scott S. K.: *J. Chem. Soc., Faraday Trans.* **1991**, *87*, 2135.
20. Koper M. T. M., Schuijff A.: *J. Phys. Chem.* **1990**, *94*, 8135.

21. Habon I., Körös E.: *Ann. Univ. Sci. Budapest, Sect. Chim.* **1979**, *15*, 23.
22. Jwo J. J., Chang E. F.: *J. Phys. Chem.* **1989**, *93*, 2388.
23. Adamčíková Ľ., Ševčík P.: *Collect. Czech. Chem. Commun.* **1987**, *52*, 2375.